Estuarine, Coastal and Shelf Science 255 (2021) 107340

Contents lists available at ScienceDirect

Estuarine, Coastal and Shelf Science

journal homepage: http://www.elsevier.com/locate/ecss

Production of methane and gaseous compounds by surface microbial activity in a small pockmark field, Dunmanus Bay, Ireland

S.S. O'Reilly [a,1], S.F. Jordan [a], X. Monteys [b], A.J. Simpson [c], C.C.R. Allen [d], M.T. Szpak [a], B. T. Murphy [a], S.G. McCarron [e], R. Soong [c], B. Wu [c], A. Jenne [c], A. Grey [a], B.P. Kelleher [a,*]

[a] School of Chemical Sciences, Dublin City University, Glasnevin, Dublin 9, Ireland
[b] The Geological Survey of Ireland, Beggars Bush, Haddington Road, Dublin 4, Ireland
[c] Department of Chemistry, University of Toronto, Scarborough Campus, 1265 Military Trail, Toronto, Canada, M1C 1A4
[d] School of Biological Sciences, Queen's University Belfast, Belfast, BT9 5DL, United Kingdom
[e] Maynooth University, Department of Geography, Maynooth, Ireland

ARTICLE INFO

Keywords:
Dunmanus
Microbial contribution.
Marine pockmarks
Cores
Biogeochemical analysis

ABSTRACT

Marine pockmarks are globally widespread seabed depressions, conventionally thought to be formed by the accumulation and expulsion of microbial and thermogenic gas. However, other putative fluids and processes have been implicated in pockmark formation and gas escape to the atmosphere may be underestimated. Given the complex spectrum of aquatic settings, morphologies and sizes, there may also exist a spectrum of physical, chemical and biological processes that form pockmarks. Pockmarks in shallow coastal waters are now understood to be widespread, but the influence of physical dynamics (e.g. tides, storms, etc.), terrestrial processes and anthropogenic activities add considerable spatiotemporal complexity and uncertainty to our understanding of these features. Here, we revisit a field of small (ca. 2 m diameter), shallow (<1 m depth) pockmarks in Dunmanus Bay, Ireland. The presence of muddy surface sediments overlying sand in the pockmarked area indicates that gas accumulation within fine-grained surface sediments contributes to formation of the features. Previous work indicates that CH_4 is an important seepage fluid in Dunmanus and neighbouring bays. However, based on evidence from multiple surveys, we observe considerable spatiotemporal complexity, and the transient nature of the gas within sediments points to the potential for fluids other than traditional microbial or thermogenic CH_4, migrating from sources tens to hundreds of metres below the seafloor. We observed atypical porewater profiles where millimolar concentrations of H_2S concentrations are observed in surface sediments in the absence of SO_4^{2-} depletion, together with NH_4^+ build-up from ammonification of sedimentary organic matter. Archaeal methanogens, anaerobic methanotrophic archaea and SO_4^{2-}-reducing Deltaproteobacteria co-occur in surface sediments in the pockmark field and NMR revealed the presence of non-competitive substrates for methanogens. We hypothesize that *in-situ* methanogenesis and production of other volatile metabolites besides CH_4 (e.g. CO_2, dimethyl disulfide) from microbial degradation of organic matter are potential gaseous fluids and could contribute to the formation of small pockmarks.

1. Introduction

Pockmarks are circular or sub-circular seabed depressions, which may reach diameters of hundreds of metres and depths of tens of metres (Judd and Hovland, 2007; King and MacLean, 1970). It is now understood that pockmarks are globally widespread, occurring in the abyssal plains and continental margins (Nelson et al., 1979; Paull et al., 2002; Picard et al., 2018; Pilcher and Argent, 2007; Skarke et al., 2014), but also in shallow coastal settings such as estuaries and bays (Brothers et al., 2011; Garcia-Gil et al., 2002; Jordan et al., 2019; Szpak et al., 2015; Wildish et al., 2008) and freshwater lakes (Pickrill, 2006; Wirth et al., 2020). Recent surveys highlight very high densities of pockmarks, or 'pockmark fields' in shallow coastal settings: for example, densities of up to 1200 km^2 in the German Bight (Krämer et al., 2017) and up to 5500 km^2 in the Bay of Concarneau, France (Baltzer et al., 2014). CH_4 migration via permeable strata and accumulation below sediments with

* Corresponding author.
E-mail address: brian.kelleher@dcu.ie (B.P. Kelleher).
[1] Current address: Department of Life Sciences, Institute of Technology Sligo, Ash Lane Bellanode, Sligo, Ireland.

https://doi.org/10.1016/j.ecss.2021.107340
Received 12 May 2020; Received in revised form 10 March 2021; Accepted 17 March 2021
Available online 20 April 2021

low permeability (clay and silt), followed by the eventual expulsion of free CH_4, interstitial water and sediment into the water column is the standard formation mechanism proposed for pockmarks (Hovland, 1989).

Sedimentary CH_4 is produced by microbial methanogenesis during degradation of organic matter, or from thermogenic gas produced by high-temperature cracking of organic matter at considerable burial depths (Reeburgh, 2007). Both microbial and thermogenic sedimentary CH_4 are consumed by microbial anaerobic oxidation of CH_4 (Boetius et al., 2000; Knittel and Boetius, 2009). Anaerobic oxidation of CH_4 manifests itself as globally widespread methane-derived authigenic carbonate (Judd et al., 2007; O'Reilly et al., 2014). Apart from being of potential interest for the oil and gas industry (Hovland, 1981) and of concern as geohazards for man-made marine installations and development (e.g. wind turbines (Coughlan et al., 2021)), there are implications for global carbon cycling since CH_4 is a major greenhouse gas. Oceanic emissions of CH_4 to the atmosphere are estimated to be 6–12 Tg CH_4 yr^{-1} (Weber et al., 2019). Although low when considering the overall CH_4 atmospheric flux from all sources - 5–20% of net modern atmospheric flux (20–100 Tg CH_4 yr^{-1}, Valentine and Reeburgh, 2000) - shallow coastal waters dominate oceanic CH_4 contributions (Weber et al., 2019). This is because CH_4 is consumed in the water column as gas bubbles rise, so seabed seepage in shallow water is more likely to be released to the atmosphere than CH_4 from deepwater pockmarks and seeps (Judd, 2004). In addition, continental margins account for approximately 90% of global sedimentary organic matter and cycling (Hedges and Keil, 1995). Thus, the recent discoveries of high densities of pockmarks in shallow (<50 m water depths) coastal settings is significant. Given the sparsity of surveys and lack of curated databases on seafloor fluid expulsion (Phrampus et al., 2020), the atmospheric flux of CH_4 and other greenhouse gases from coastal marine settings could be substantially underestimated.

There is further uncertainty around pockmarks because other mechanisms including non-hydrocarbon fluids have also been implicated in pockmark formation: CO_2 (Stott et al., 2019), compaction of pore water (Harrington, 1985), groundwater seepage (Christodoulou et al., 2003; Wirth et al., 2020), iceberg scouring (Pilcher and Argent, 2007), anthropogenic activities such as trawling (Fader, 1991) and biological activity (Szpak et al., 2012). Thus, significant questions remain regarding the formation, longevity and extent of atmospheric greenhouse gas emissions from the thousands of shallow pockmarks in existence today.

In this study, we returned to a small pockmark field in Dunmanus Bay, South-West Ireland, originally identified in 2007 during a multibeam mapping survey carried out by the RV Celtic Voyager as part of the Integrated Mapping For Sustainable Development of Ireland's Marine Resources (INFOMAR) programme. Based on the data collected in 2009, Dunmanus Bay pockmark field consists of 121 circular, shallow units ranging from 5 to 17 m in diameter and not exceeding 1 m in relief (Szpak et al., 2015). Acoustic signatures revealed shallow gas accumulation in the subsurface and signals of ascending bubbles were captured in echo sounder data. Pockmark features closely correlated with concentration of sub-surface CH_4 but CH_4 concentrations in the water column directly above the features were close to typical background values suggesting mild periodic venting. No evidence of freshwater was found indicating that CH_4 gas is the main fluid involved in pockmark formation. We revisited the site in 2013 and carried out a multidisciplinary investigation of sediment cores from pockmarked and non-pockmarked sediments within the Dunmanus Bay pockmark field, and surrounding areas. Our aim was to investigate CH_4 seepage and study potentially distinct microbial processes in this shallow pockmark site.

1.1. Environmental and geological setting

Dunmanus Bay is in southwest Ireland and is 7 km wide from Sheep's Head to Three Castles Head and 25 km long from its mouth (Fig. 1). It is a rias setting with only one small river, the Durrus, and several streams draining into the bay. Water depth ranges from below 20 m in the inner bay to over 70 m at its mouth. The area is strongly influenced by coastal upwelling but tidal activity is low as Dunmanus Bay is out of the main tidal flow (Edwards et al., 1996). The in-depth environmental and geological setting is reported by Szpak et al. (2015). Core sampling (below) was guided by previously reported detailed multibeam bathymetric mapping and backscatter mapping of pockmarks and sub-bottom acoustic profiling for acoustic turbidity. Acoustic turbidity - chaotic seismic facies masking nearly all other reflections - can be caused by gravel or sand beds or from interstitial gas bubbles in the sediment (Missiaen et al., 2002; Schubel, 1974). Geophysical studies in Dunmanus

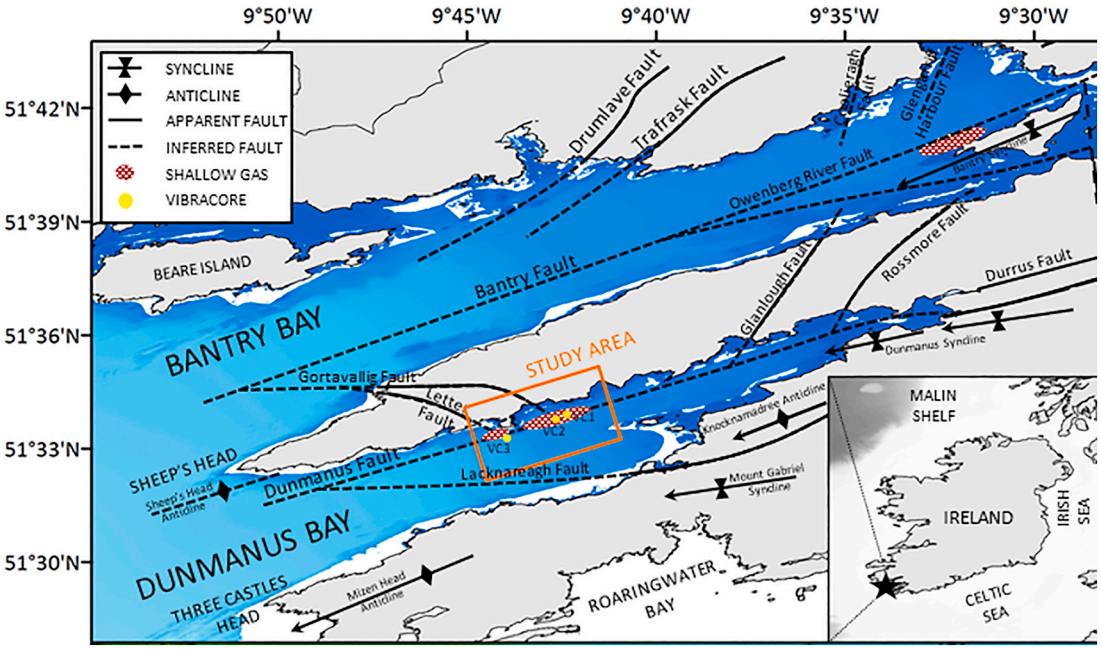

Fig. 1. Dunmanus Bay map showing the location and outline of Dunmanus Bay pockmark field (shallow gas) and core sampling points. Bathymetry, structural features, major faults and pockmark field are shown in greater detail in Szpak et al. (2016) [18].

and neighbouring Bantry Bay have identified interstitial gas as the main source of acoustic turbidity. Ground-truthing has demonstrated millimolar concentrations of CH_4 in subsurface sediments in Bantry Bay (Jordan et al., 2019) and bubbles seeping from the water column at Dunmanus Bay (Szpak et al., 2015).

2. Materials and methods

2.1. Core sampling

Based on previous geophysical surveys and ground-truthing (Jordan et al., 2019; Szpak et al., 2015), three 6 m vibrocores were collected in 2011 using a GeoResources Geo-Corer 6000 aboard the RV Celtic Explorer (CE11_017). One core was sampled from a composite pockmark with evidence of shallow subsurface acoustic turbidity (VC1; Latitude: 51.5590, Longitude: −9.7130), one from sediments exhibiting previous evidence of acoustic turbidity, but which was non-pockmarked sediment (VC2; Latitude, Longitude: 51.5600, −9.7101) and one core was sampled from typical marine sediment at 1.5 km to the southwest of the pockmark field (VC3; Latitude, Longitude: 51.5513, −9.7322).

10 mL sediment plugs were sampled from windows cut in the core liner, transferred to a 20 mL headspace vial and 1.2 M NaCl solution containing approximately 70 mg L^{-1} thimerosal ($C_9H_9HgNaO_2S$, Sigma Aldrich, Dorset, UK) was then added to the vial leaving a 3 mL headspace. Sealed vials were stored in the dark at 4 °C prior to analysis back in the laboratory. Between 3 mL and 10 mL of porewater was subsampled from core liner windows using Rhizon samplers (Rhizosphere Research Products, Wageningen, NL). 1 mL aliquots for H_2S analysis were preserved by addition of 400 μL 50 mM $Zn(CH_3CO_2)_2$. 1 mL aliquots were preserved with 1–2 drops of chloroform for PO_4^{3-} and NH_4^+ analysis. Sediment sub-samples were taken from working sections after gas and porewater sampling, and stored onboard at −20 °C, and at −80 °C back in the laboratory. Sub-samples for bulk chemical and physical parameters were stored at 4 °C.

2.2. Gas and porewater analysis

CH_4 analysis was performed on an Agilent 7820A gas chromatograph with a flame ionisation detector with a 30 m HP-PLOTQ column (Agilent, Santa Clara, USA). Column conditions were isothermal (50 °C). CH_4 was quantified using calibration standards prepared from a 99.995% CH_4 standard (Sigma Aldrich, Dorset, UK). Analytical precision was calculated to be between 5 and 10% ($[\sigma \times 100]/\bar{x}$, where σ is the standard deviation of the peak areas and $\bar{x}$ is the mean of the peak areas for replicates of a standard concentration). Selected gas samples were sent to Woods Hole Oceanographic Institute for stable carbon isotope analysis of CH_4 ($^{13}C_{CH4}$). Triplicate analyses were performed on all gas samples. Isotope data are reported in the "del" notation (i.e., $\delta^{13}C$):

$$\delta = 1000[(R_{sam} / R_{std}) - 1)]$$

where R_{sam} is the isotopic ratio ($^{13}C/^{12}C$) of the sample and R_{std} is the isotopic ratio of the referenced standard (Pee Dee belemnite (PDB)). The units of δ are permil (‰). The analytical errors for stable isotopic analyses are ±0.4‰ for $\delta^{13}C_{CH4}$.

Spectrophotometric analysis of H_2S was performed using leucomethylene blue (Cline, 1969). Spectrophotometric analysis of PO_4^{3-} was performed using phosphomolybdate complexation (Towns, 1986). Analysis for both H_2S and PO_4^{3-} was conducted on a BIOTEK Powerwave HT plate reader and calibration standards were prepared in artificial seawater prepared from commercially available sea salts (Sigma Aldrich, Dorset, UK). H_2S and PO_4^{3-} analytical precision was calculated to be between 1 and 5%. NH_4^+ analysis was performed using a SCHOTT NH1100 ion selective electrode and using manufacturer calibration solution and ion strength adjustment buffer (Reagecon, Clare, Ireland). Calibration and quantification was performed according to manufacturer guidelines but scaled down to analysis of 1 mL water aliquots. SO_4^{2-} was determined by suppressed ion chromatography on a DX-120 Dionex Ion Chromatograph with an eluent generator (K_2CO_3) and an anion exchange column (IonPak AS18). The mobile phase was Nanopure grade water (18MΩ), which was automatically amended with hydroxide ions to a preset concentration (15 mM OH^-). The mobile phase flow was set to 1.0 ml min^{-1} and suppressor current was set to 25 mA. Data processing and peak integration was conducted using the Chromelion software package. Analytical precision was calculated to be <8% based on duplicate analysis of standards and samples.

2.3. Bulk physical and chemical analysis

Particle size analysis was performed using laser granulometry (Malvern MS2000) for sediment fractions <1000 μm and dry sieving for fractions >1000 μm. Percentage per size class calculated using the MS2000 were converted to total sample percentages and integrated with the >1000 μm data. Total organic carbon and total nitrogen was analysed using an Exeter Analytical CE440 elemental analyser, after oven-drying and removal of inorganic carbonate using 1 M HCl. Loss-On-Ignition was determined in higher resolution by combusting 300–500 mg oven-dried sediment to constant weight at 440 °C for 8 h in a muffle furnace.

2.4. 16S rRNA gene profiling of microbial diversity

DNA was extracted using the POWERSOIL DNA isolation kit (MO BIO, Carlsbad, US) according to manufacturer guidelines. Barcoded bacterial 16S rRNA gene pyrosequencing was carried out on 9 samples according to (Berry et al., 2011) and as previously described (O'Reilly et al., 2016). During polymerase chain reaction (PCR), long oligonucleotides consisting of the gene-specific PCR primer sequences tagged with the sequencing adapters for GS FLX Titanium chemistry were used and the reverse primer included an 8 base pair barcode identifier (Hamady et al., 2008). Archaeal 16S rRNA gene pyrosequencing was carried out on two samples (VC1 1.3 m and VC2 1.3m) using the same approach but using the established archaeal Arch-21F and Arch-958R primers (Vetriani et al., 1999). Purified amplicons of known concentration were submitted to the sequencing facility in the Department of Biochemistry, Cambridge University (UK), where pyrosequencing was performed using a Roche 454 Junior sequencer (detailed in SI methods). For the resulting amplicon dataset, distance matrices between samples were determined using the Bray-Curtis dissimilarity index (Vigneron et al., 2017). Statistical analysis was performed using PAST Software v4.03 (Hammer et al., 2001). All sequences have been uploaded to NCBI under BioProject accession number PRJNA717047.

2.5. Sedimentary organic matter composition

Sedimentary organic matter was isolated according to previously described methods (Gonçalves et al., 2003). Freeze-dried sediment (ca. 120 g accurately weighed) was extracted with deionized water (x3). Organic matter was concentrated, and ferromagnetic minerals removed by shaking samples overnight in 10% 1:1 (v/v) HCl/HF (x2), followed by 10% HF (x8). Concentrated organic matter was then exhaustively extracted with 0.1 M NaOH. Water and NaOH extracts were centrifuged and supernatants were filtered through 0.22 μm polyvinylidene fluoride membrane filters (Merck Millipore, Billerica, USA). Water extracts were combined and dried by rotary evaporation and stored at −80 °C. NaOH extracts were ion-exchanged using AMBERJET 1200H cation exchange resin to remove Na^+ ions. NaOH extracts were subsequently freeze-dried and all extracts were desiccated for 48 h prior to further analysis.

Each sample (40 mg) was resuspended in 1 mL of D_2O and titrated to pH 13 using NaOD (40% by wt) to ensure complete solubility. Samples were analysed using a Bruker Avance 500 MHz NMR spectrometer equipped with a ^1H–^{19}F–^{13}C–^{15}N 5 mm, quadrupole resonance inverse

probe fitted with an actively shielded Z gradient. 1-D solution state ^{1}H NMR experiments were performed at a temperature of 298 K with 128 scans, a recycle delay of 3 s, 16,384-time domain points, and an acquisition time of 800 ms. Solvent suppression was achieved by pre-saturation utilising relaxation gradients and echoes (Simpson and Brown, 2005). Spectra were apodised through multiplication with an exponential decay corresponding to 1-Hz line broadening, and a zero-filling factor of 2. Diffusion-edited experiments were performed using a bipolar pulse longitudinal encode-decode sequence (Wu et al., 1995). Scans (n = 1024) were collected using a 1.25 ms, 52.5 G cm^{-1}, sine-shaped gradient pulse, a diffusion time of 100 ms, 16,384 time domain points and 819 ms acquisition time. Spectra were apodised through multiplication with an exponential decay corresponding to 10 Hz line broadening and zero-filling factor of 2.

2.6. Porewater dissolved organic matter composition

At least 10 mL aliquots of selected porewater samples were additionally filtered through 0.22 μm Polyvinylidene fluoride membrane filters and dissolved organic matter was subsequently preserved in sodium azide (final concentration of 0.1%). All NMR experiments were carried out according to (Lam and Simpson, 2008) on a Bruker Avance 500 MHz equipped with a 5 mm ^{1}H-BB-^{13}C TBI probe with an actively shielded Z-gradient. 1D solution state 1H NMR experiments were acquired with a recycle delay of 2 s, and 32,768 time domain points. Spectra were apodised by multiplication with an exponential decay producing a 10 Hz line broadening in the transformed spectrum, and a zero-filling factor of 2. Where appropriate, pre-saturation was applied on resonance generated by a 60 W amplifier attenuated at 50 dB during the relaxation delay. Direct ^{1}H NMR was performed using WATER suppression by GrAdient-Tailored Excitation (WATERGATE) and was carried out using a W5 train and a 125 μs binomial delay such that the 'sidebands' occurred at ca. 12 ppm and 2 ppm and were outside the spectral window. W5-WATERGATE was preceded by a train of selective pulses: 2000, 2 ms, calibrated π (180°) pulses were used, each separated by a 4 μs delay.

3. Results

3.1. Lithology

Sediment core VC1 consisted of poorly sorted mud (average silt content 74.2%) in the top 150 cm, followed by a sharp transition to poorly sorted/very poorly sorted sandy mud to 3 mbsf (Fig. 2). Below 3 mbsf, sediment coarsens to muddy sand, before a sharp transition to gravel at approx. 4 mbsf. Below 4 mbsf, sediment was well sorted sand. VC2 contained lower clay and higher sand content, and overall a more variable lithology in the first 2 mbsf compared to VC1. Below about 2 mbsf, VC1 and VC2 grain and sediment type are similar, while VC3 was dominated by quite homogeneous sandy sediment throughout, apart from a surface layer of shell, shell-hash and organic detritus. In all three cores a distinct gravel stratum was observed at about 4 mbsf, and is the source of the enhanced reflector in acoustic profiles (Szpak et al., 2015). The occurrence of finer-grained muddy sediment coincides with the highest concentrations of organic matter (Fig. 2 and Supplementary Information).

3.2. Porewater and CH_4 geochemistry

Geochemical profiles for VC1, VC2 and VC3 are presented in Fig. 2. Due to the compaction caused by vibrocore sampling and the potential for vibrations to disturb the sediment-water interface, geochemical zonation across the sediment-water interface and to an estimated depth of about 10 cm below the seafloor are likely disturbed. Sediment pushcores were not taken during this survey to complement our vibrocore data. As in 2009 (Szpak et al., 2015), interstitial CH_4 concentrations were in the low micromolar range in both VC1 and VC2 in 2011. Interstitial CH_4 concentrations were negligible below 3 mbsf in the sandy strata in VC1 and VC2 and throughout the core at VC3. $\delta^{13}C_{CH4}$ values were obtained for 0.5 m core depth in VC 1 and for 1.85 and 2.0 m core depth in VC2. The VC1 samples measured −77‰, while the samples from VC2 measured −49‰ and −50‰ respectively.

Millimolar (up to 2.2 mM) concentrations of H_2S were detected in porewater collected from the upper muddy sediment in VC1 and VC2. H_2S was negligible in deeper sands and throughout VC3. H_2S concentrations were higher closer to the seafloor in VC2 (1.2 mM) compared to VC1 (0.4 mM). NH_4^+ concentrations increase linearly with depth in both VC1 and VC2, but concentrations were between 2 and 3 times higher for the upper 3 mbsf in VC2. NH_4^+ concentrations in VC3 were substantially lower than VC1 and VC2. PO_4^{3-} profiles for VC1 showed maximum concentrations around 0.7 mbsf to 1.25 mbsf, after a comparatively sharp increase from close to the sediment-water interface, while in contrast maximum PO_4^{3-} concentrations were detected close to the sediment-water interface in VC2 (and a clear linear decreasing trend with depth). PO_4^{3-} concentrations in VC3 were as much as an order or magnitude lower than VC1 and VC2.

3.3. Microbial community composition

Phylogenetic analysis of 16S rRNA gene sequences showed clear differences in bacterial communities at the phylum to genus level in surface sediments between mud and sand, and between mud within the Dunmanus Bay pockmark field (Fig. 3). Cluster analysis of Operational Taxonomic Unit's (OTUs; Fig. 3B) shows that bacterial populations in surface sediment at VC3 were most distinct, followed by the bacterial population at 1 mbsf depth in VC2. The bacterial populations at 0.1 and 2 mbsf in VC2 and 1 and 2 mbsf in VC1 formed a cluster with 79% similarity.

In the pockmark field, most sequences were affiliated with Planctomycetes (33% on average), followed by Proteobacteria (13%), candidate CD12 (8%), GN04 (8%), OP8 (6.6%), OP9 (5.2%), Bacteroidetes (4.5%) and OD1 (3.7%). In contrast, in VC3 Proteobacteria dominated (23%), followed by Planctomycetes (18%), Bacteroidetes (11%), CD12 (5%), GN04 (4%), OP8 (3%), OP11 (2.4%), Verrucomicrobia (2.3%), Elusimicrobia (2%), Actinobacteria (2%) and Acidobacteria (1.9%). In total uncultured candidate phyla accounted for between 33 and 45% of all sequences, apart from at 1 mbsf in VC2 (20%) and 0.1 mbsf in VC3 (3%). Few sequences could be assigned to known taxa at greater than the phylum level. However, 12% of sequences from 0.1 mbsf in VC1 and from 1.0 mbsf in VC3 were affiliated to *Desulfobacteraceae* (12%). 7% of sequences at 1.0 mbsf in VC2 clustered within *Desulfobulbaceae* and 20% of the sequences at 0.1 mbsf in VC3 were related to *Flavobacteriaceae.*

Archaeal community composition and diversity was investigated in two sub-bottom samples, from VC1 and VC2 at 1.3 m core depths. These coincided with the highest concentrations of CH_4. Thermoplasmata OTUs accounted for 44% and 25% of 16S rRNA genes at VC1 and VC2 (respectively), while the candidate Miscellaneous Crenarchaeota group (MCG) represented 35% and 26% of VC1 and VC2 archaeal 16S rRNA genes. Marine Benthic Group B (MBGB) was the only other archaeal OTU that represented greater than 4% of 16S rRNA archaeal genes (14% of total), while Thaumarchaeota and an unclassified OTU were other major OTU groups in VC2 (7% and 21%, respectively). Methanobacteria represented 1.1% of archaeal 16S rRNA genes in VC1 but 2.1% in VC2 and anaerobic methanotrophic (ANME) archaea from the clades 1 (ANME-1) were only detected in VC2 (1% of archaeal 16S rRNA genes).

3.4. Characterization of sedimentary organic matter

Alkaline extracts of sediment from four depths from each core were analysed by ^{1}H-NMR to characterize sedimentary organic matter composition (Fig. 4). The 0.75–2.5 ppm region contains aliphatic and amino acid side chain signals and signals for carbohydrates and O-alkyl

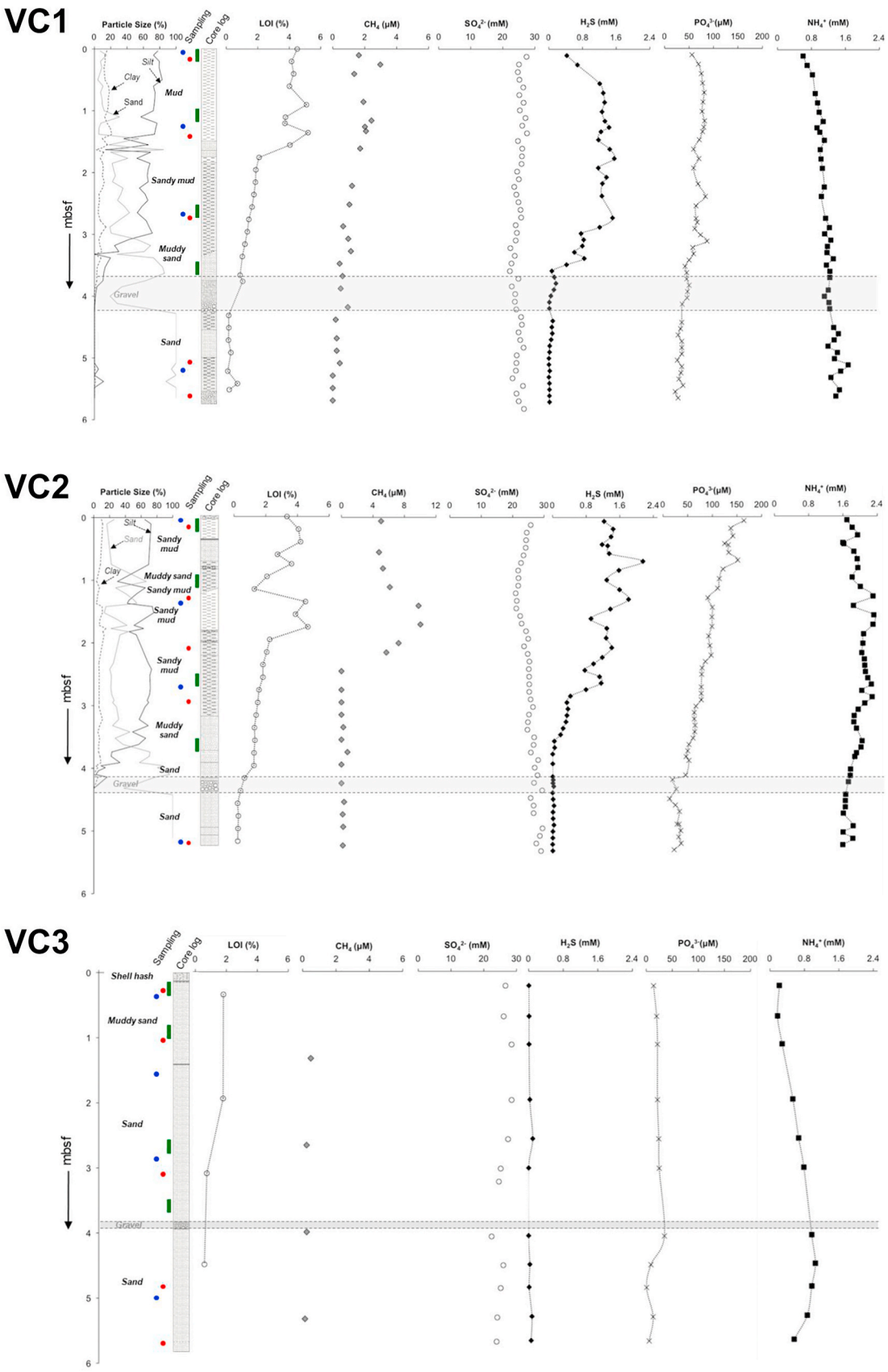

Fig. 2. Downcore profiles of physical and chemical parameters from core VC1, VC2 and VC3. Blue circles – Lipid and DNA sampling, red circles – porewater NMR sampling, green boxes – sedimentary NMR sampling.

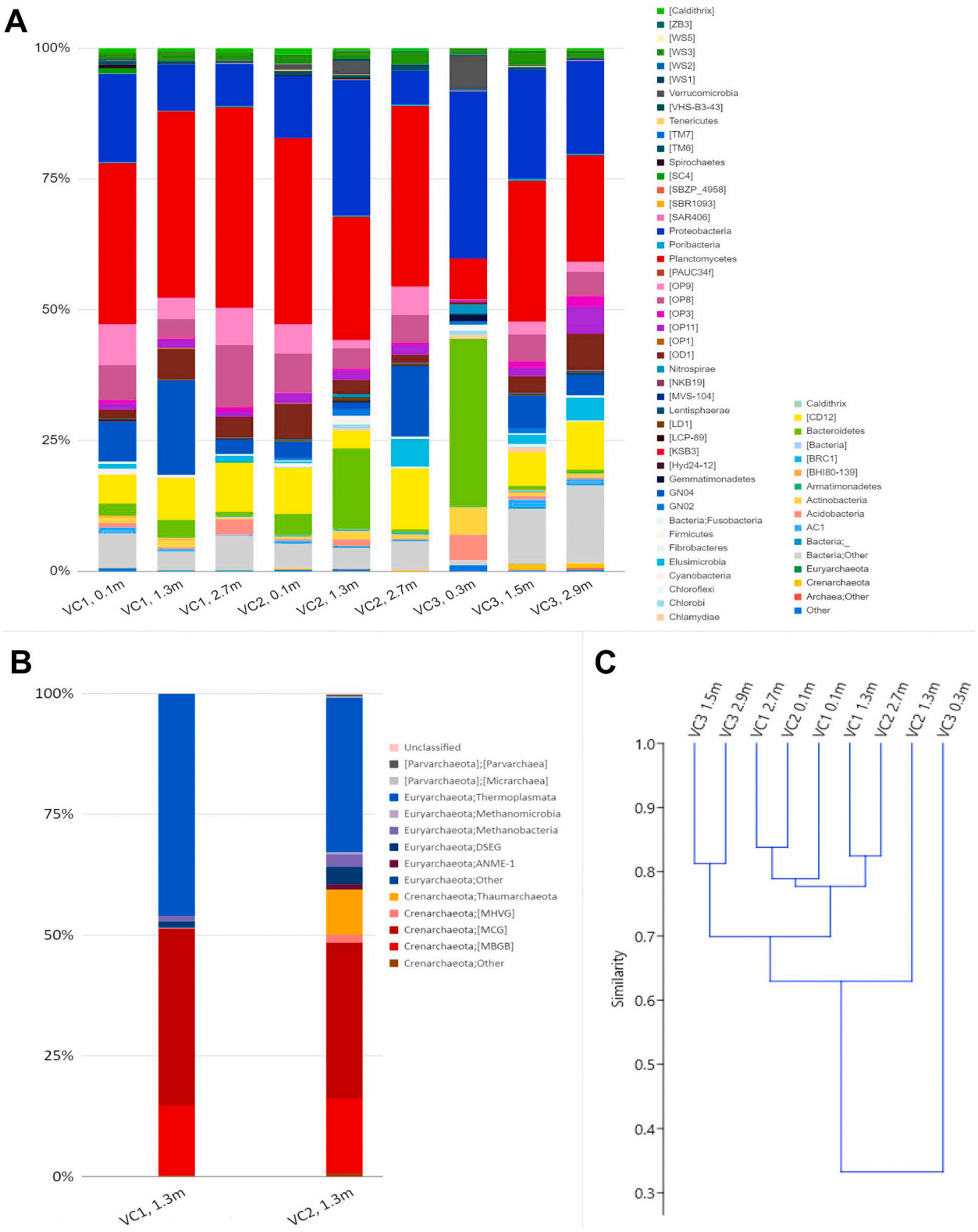

Fig. 3. 16S rRNA gene 454-pyrosequencing of bacterial (A) and archaeal (B) community composition and hierarchical cluster analysis (beta-diversity, C).

groups on amino acids exist in the 3.5–4.5 ppm region. The abundance of carbohydrate resonances and broader unresolved peaks in the surface spectra of VC1 and VC2 reflects a larger input of OM in this area from both allochthonous and autochthonous sources compared with the surface sediments around VC3. This is also reflected in bulk Loss-On-Ignition profiles (Fig. 2). The amount of labile organic matter, based on the region characteristic of carbohydrates and amino acids, decreases from the surface to ca. 1 mbsf in both VC1 and VC2, while only slight differences were observed for VC3. Protons associated with *N*-acetylmuramic acid – one of the primary constituents of the bacterial cell wall polymer, peptidoglycan – are based on the characteristic resonance peak for the *N*-acetyl functional group at 2.03 ppm, as previously

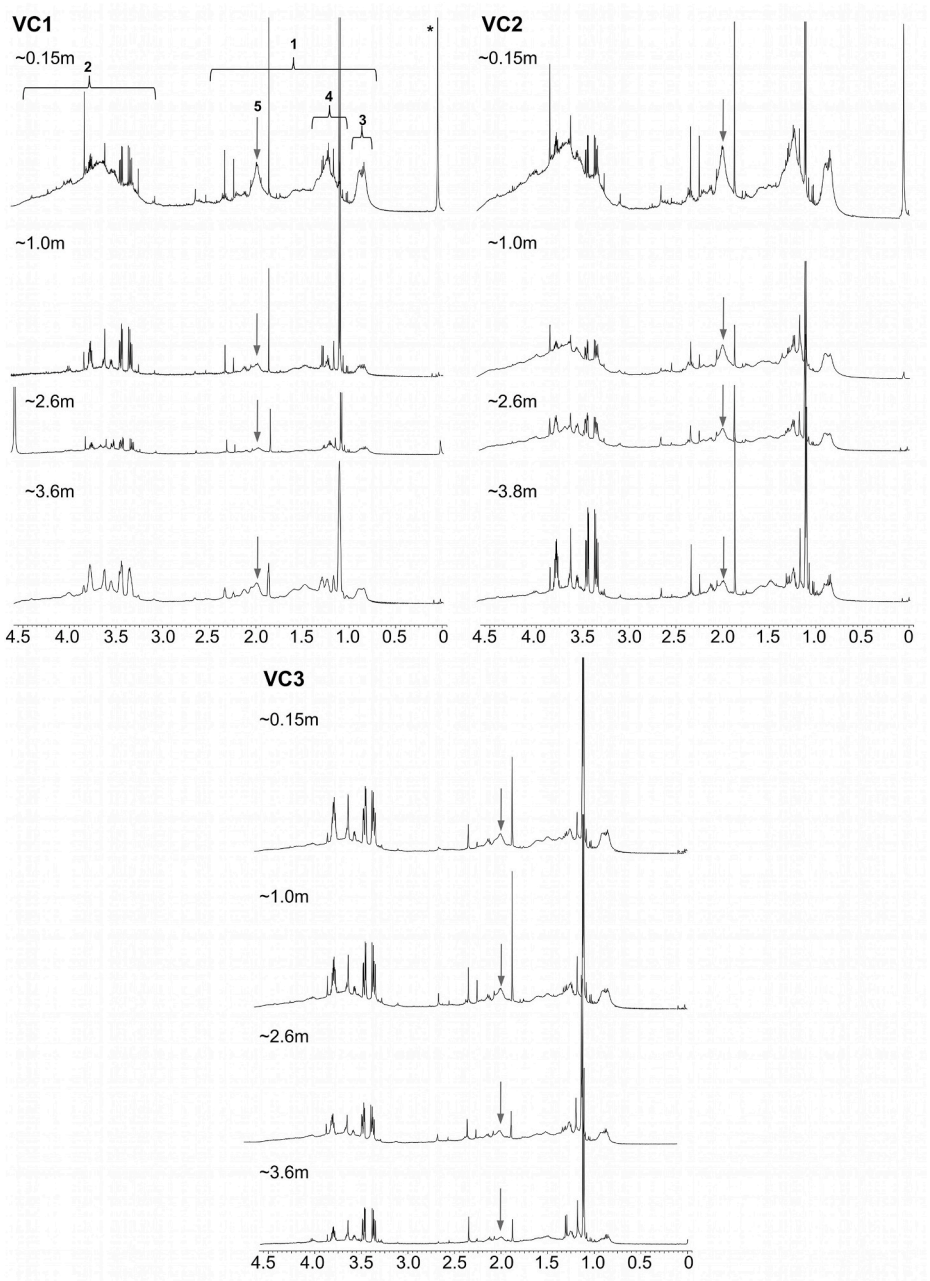

Fig. 4. Partial 1D ^{1}H NMR spectra from NaOH extracts. General region assignments correspond to aliphatics (1) - signals from various substituted methylenes, and methanes β to a functionality in hydrocarbons (signals from some amino acid side chains will also resonate here), carbohydrates and amino acids (2) – signals from protons α to O-alkyl functional groups. More specific assignments are protons associated with CH_3 groups in amino acid side chains (3), protons associated with methylene groups in aliphatic compounds (4), protons associated with N-acetyl functional groups in peptidoglycan (5) and protons associated with naturally occurring silicates compounds (*). The grey arrow highlights the resonance peak associated with peptidoglycan.

described (Szpak et al., 2012).

3.5. Characterization of the porewater dissolved organic matter

Direct NMR analysis of porewater was performed to investigate microbially-mediated reactions between sedimentary aqueous and solid phases (Fig. 5). Specific spectral characteristics in the chemical shift region from 1.7 to 3.3 ppm are present in a majority of ^{1}H NMR spectra for both marine and freshwater dissolved organic matter, and attributed to a complex mixture of compounds known as carboxyl-rich alicyclic molecules (CRAM) (Hertkorn et al., 2006; Lam et al., 2007). CRAM is now recognized as a major refractory component of global marine and freshwater dissolved organic matter derived from terpenoids with carboxyl-to-aliphatic carbon ratios of approximately 1:2 to 1:7 (Lam et al., 2007). Interestingly, the classic "hump" in this region of the spectrum for CRAM is not prevalent on any of the core samples indicating that down-core, porewaters do not share the same chemical properties as globally consistent dissolved organic matter. Nevertheless, the porewater spectra illustrate the presence of a complex mixture of organic matter where the highest relative abundance of total dissolved organic matter resides in VC1 and VC2 in the first 1 m and a comparable composition between cores in deeper sandy strata. A range of volatile organic acids and microbial metabolic end-products were identified in porewater ^{1}H NMR spectra (Fig. 5), including acetic acid, formic acid, lactic acid and pyruvic acid.

4. Discussion

4.1. Microbial activity and biogeochemical cycling in Dunmanus Bay pockmark field

During decomposition of complex organic nitrogen compounds (e.g. proteins, nucleic acids), amino acids are mineralized to NH_4^+ via microbial ammonification (Froelich et al., 1979). In combination with

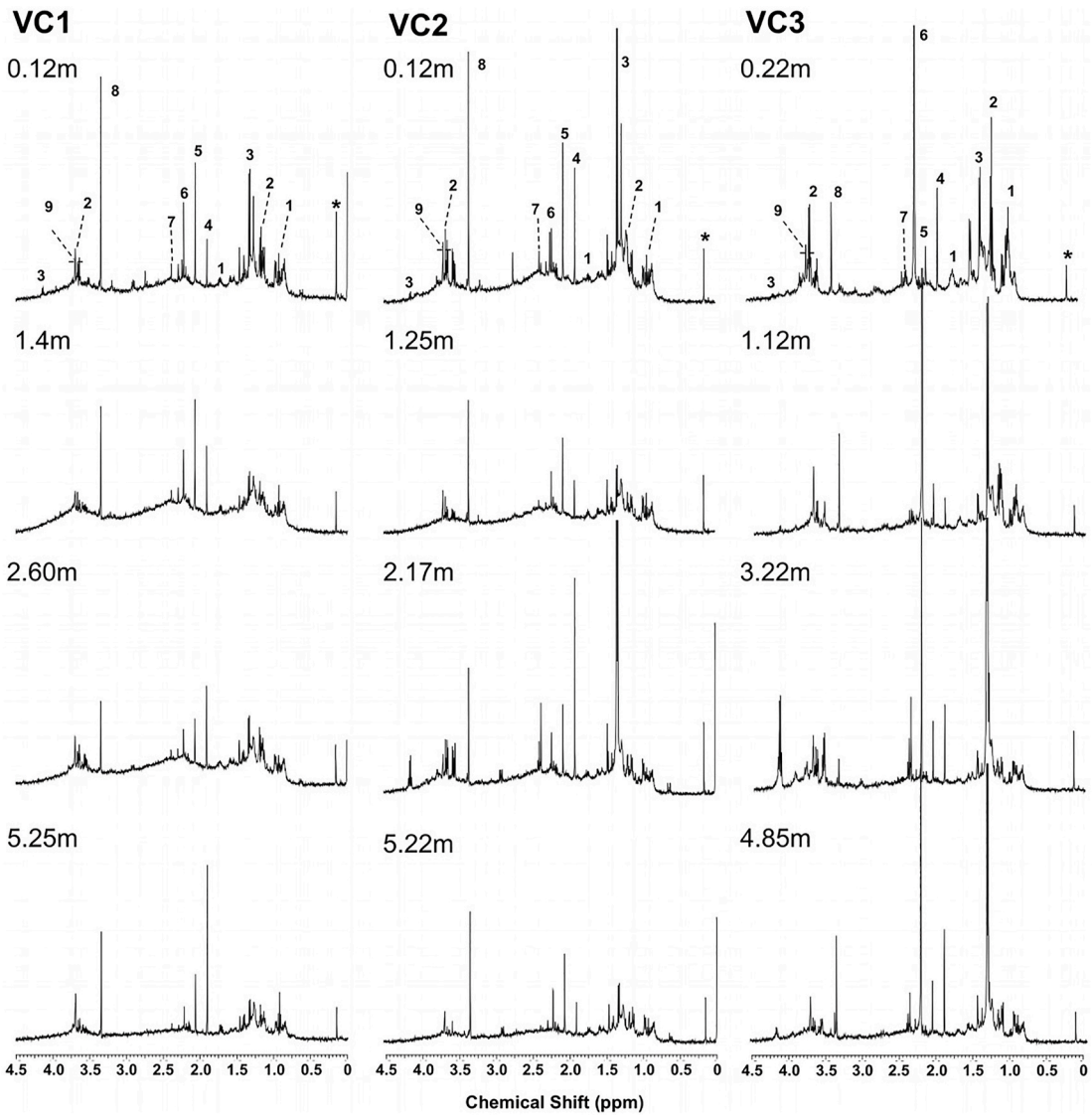

Fig. 5. 1D water-suppressed ^{1}H NMR spectra of porewater dissolved organic matter from selected depths in VC1, VC2 and VC3. Specific assignments correspond to leucine (1), ethanol (2), lactic acid (3), acetic acid (4), dimethyl sulphide (5), acetone (6), pyruvate (7), methanol (8) and glycerol (9). Tyrosine, phenylalanine and formate were also identified in the 6.8–8.5 ppm region but are not included for clarity.

microbial N_2 fixation and dissimilatory nitrate reduction to ammonium (Gardner et al., 2006; Giblin et al., 2013), and in the absence of biological or physicochemical removal of NH_4^+, microbial ammonification can accumulate NH_4^+ up to several millimolar in porewater (Batley and Simpson, 2009). While the sediment-water interface may not have been preserved, our combination of porewater data indicates rapid accumulation of >1 mM NH_4^+ within at least the first 10 cm of the seafloor. The surface 3 m of pockmark and nearby muddy sediment also displayed PO_4^{3-} porewater profiles that were very different to the control site. In shallow marine sediment, PO_4^{3-} in porewater reflects microbial degradation of protein and generally active microbial metabolisms (released from adenosine triphosphate). Porewater PO_4^{3-} also tends to become more concentrated with depth, reaching levels of up to several hundred micromolar. This scenario depends on several factors such as the type and rate of organic matter supply (Schulz et al., 1994). Porewater and sediment NMR provide an opportunity to study the metabolic products from microbial metabolisms in the Dunmanus Bay pockmark field and degradation stage of different classes of organic matter. Our NMR data show that labile organic matter is deposited in surface sediments but is readily decomposed, based on the loss of solid phase sedimentary organic signals with depth and the presence of amino acids (leucine, tyrosine, phenylalanine) as major components of porewater dissolved organic matter. Peptidoglycan is a major component in bacterial cell membranes and the higher relative abundance of peptidoglycan in VC2 suggests a higher abundance of bacterial-derived organic matter in VC2 (Kelleher et al., 2007; Simpson et al., 2007).

SO_4^{2-} reduction and H_2S production in marine sediments is generally linked by the process of dissimilatory SO_4^{2-} reduction (Jørgensen, 1977). The presence of millimolar concentrations of H_2S in VC1 and VC2 without substantial observed SO_4^{2-} depletion indicates that H_2S in Dunmanus Bay has several sources and is not efficiently removed from porewater. SO_4^{2-}-reducing bacteria, particularly *Desulfobacteraceae*, were major OTUs at all depths in all cores, including surface samples, indicating SO_4^{2-} reduction is still a significant process in the muddy surface sediments near the pockmark field. H_2S is typically precipitated as pyrite or re-oxidized to SO_4^{2-} (Jørgensen, 1982). In all cores, shallow muddy sediments were olive-green to grey in colour and did not exhibit reduced black sediments typical of pyrite precipitation. In the neighbouring Bantry Bay, millimolar concentrations of H_2S were also observed in sediments in the presence of SO_4^{2-} (Jordan, unpublished results), indicating this may be typical of sediments in this region. Although we did not measure porewater Fe species (e.g. Fe^{2+}) or solid phase mineralogy,

it is likely that Fe_xO_y minerals are not dominant or that the rate of Fe^{2+} supply is insufficient to remove porewater H_2S as solid FeS, FeS_2 or other FeS minerals.

Acetic, formic, lactic and pyruvic acid were detected as major components of porewater and are important intermediate products of the anaerobic metabolism of higher molecular weight organic matter to CH_4 and CO_2 (Sansone and Martens, 1982; Sørensen et al., 1981). Their accumulation in porewater, together with the NH_4^+, H_2S and PO_4^{3-} porewater profiles we observed, indicates the surface muds associated with the pockmark field quickly become oxygen-depleted and are dominated by anaerobic processes. Bacterial communities were dominated by candidate bacterial phyla, with no cultured representatives. As such, limited insights can be gleaned about the metabolic potential and biogeochemical impact of these taxa. 16S rRNA genes for Candidate Phylum (OP8), occur in diverse settings, with high relative abundance (2–10% of total bacterial 16S rRNA genes) in groundwater, hydrothermal vents, coral microbiomes and anoxic marine and freshwater environments (Farag et al., 2014). The OP9 (or 'Atribacteria') lineage were also abundant in Dunmanus; comparative genomic analysis has revealed that members of OP9 are likely to be heterotrophic anaerobes that lack respiratory capacity, with some lineages predicted to specialise in either primary fermentation of carbohydrates or secondary fermentation of organic acids, such as propionate (Nobu et al., 2016). Candidate CD12 ('Aerophobetes') may be facultative anaerobic, potentially more closely associated with cold seeps (Wang et al., 2016), although currently only described in deep-sea sediments. SO_4^{2-}-reducing clades within the class Deltaproteobacteria were also abundant, and are predominantly anaerobic bacteria involved in sulfur cycling (Anantharaman et al., 2018; Miyatake et al., 2009).

The major archaeal clades in Dunmanus Bay pockmark sediments were the Miscellaneous Crenarchaeotic Group (MCG), the Deep-Sea Hydrothermal Vent Euryarchaeotic Group I (DHVEG-1, within the class Thermoplasmata) and the crenarchaeotal marine benthic group-D (MBG-D). Based on the evidence available, these clades appear to be very cosmopolitan generalist sedimentary archaea (Cao et al., 2015; Fillol et al., 2016; Lloyd et al., 2013). MCG and MBG-D appear to play a key role in protein remineralization in anoxic marine sediments (Lloyd et al., 2013). Several OTUs were related to clades known to be involved in methanogenesis or anaerobic oxidation of CH_4. *Methanomassiliicoccaceae* (Thermoplasmata) accounted for 1.2% of archaeal 16S rRNA genes in VC2 but were not detected in VC1; evidence to date indicate that archaea in this clade are methylotrophic methanogens, whereby they produce CH_4 from methylated compounds like methanol (CH_3OH) and methanethiol (CH_3SH) (Vanwonterghem et al., 2016). These clades could produce CH_4 at or above the SO_4^{2-}/CH_4 transition zone, in the presence of SO_4^{2-} (Lazar et al., 2012; Oremland et al., 1982). ANaerobic MEthanotropic (ANME) archaea clade 1 (ANME-1) are well established uncultured microorganisms associated with anaerobic oxidation of CH_4 in marine sediments (Boetius et al., 2000) and also capable of methanogenesis (Lloyd et al., 2011). The occurrence of ANME-1 suggests anaerobic oxidation of CH_4 was occurring in VC2 at 1.3 mbsf at the time of sampling but not at VC1. Overall, 16S rRNA data suggest methanogenesis and anaerobic oxidation of CH_4 to CO_2 was occurring in VC2, within non-pockmarked sediment in the pockmark field but not in the sampled pockmark clusters (VC1).

4.2. Lithological controls on sediment biogeochemistry in Dunmanus Bay

The presence of CH_4 at low micromolar concentrations in sediments within the Dunmanus Bay pockmark field in 2011 (this study) and in 2009 (Szpak et al., 2015) suggest that: sub-bottom acoustic evidence for gas (acoustic turbidity, blanking etc.) is caused by features other than gas, both sampling surveys occurred during a period of low CH_4 accumulation in sediments or that acoustic features were caused by fluids other than CH_4 (e.g. CO_2, freshwater etc.). Evidence of groundwater discharge is lacking from multiple surveys to date as evidenced by seawater concentrations of major anions in porewater profiles. The presence of gas bubbles in the water column above the Dunmanus Bay pockmark field previously (Szpak et al., 2015) and confirmation of high production and consumption of CH_4 in the neighbouring Bantry Bay (Jordan et al., 2019), point towards gas rather than groundwater or porewater as the fluid responsible for pockmark formation in this region.

Differences in permeability is a major control on fluid and solute transport in sediments, and the degree of sediment-water column exchange of solutes and particles (Huettel et al., 1998). In addition, the interface between sediment particles and porewaters are key sites of biogeochemical processes and microbial activity. In this way, lithology and particle size are major controlling factors governing geochemical zonation and associated microbial population structure (Santos et al., 2012; and references therein). As for other locations with pockmarks, hydrodynamic conditions and resulting favourable deposition of fine-grained muddy sediment is a major factor governing the distribution of pockmarks (Jordan et al., 2019; Szpak et al, 2012, 2015). The rapid loss of H_2S and CH_4 from sandy sediments at depth in the cores indicates transport of oxygenated seawater in permeable sands and gravel layers below the muddy surface sediment below Dunmanus Bay pockmark field. We observed similar SO_4^{2-} reduction in the Dunmanus Bay pockmark field in the first 1 m before increasing again with depth (Szpak et al., 2015). The consistent higher concentration of CH_4, NH_4^+, PO_4^{3-} and the increased relative abundance of methanogens and anaerobic methanotrophic archaea at the non-pockmarked VC2 site compared the pockmarked VC1 site suggests higher microbial activity in sediments surrounding the formed pockmarks in Dunmanus Bay pockmark field.

4.3. In-situ sedimentary microbial production of gaseous metabolites

While gas is the most likely fluid involved in pockmark formation in Dunmanus Bay, the source of this gas is not well constrained. In the conventional model, when microbial or thermogenic CH_4 exceeds the capacity of interstitial water to take it into solution, free CH_4 gas bubbles develop in the pore spaces, building pressure in the relatively impermeable sediments (Hedberg, 1980). Thermogenic CH_4 typically exhibits $\delta^{13}C_{CH4}$ of −20 to −50‰ while microbial CH_4 is typically characterized by lighter carbon and $\delta^{13}C_{CH4}$ of −50 to −110‰ (Stolper et al., 2015; Whiticar, 1999). While this suggests that CH_4 in VC1 and VC2 are from different end-member sources, additional analysis of the dD-CH_4 would be needed to confirm this. Microbial CH_4 production is conventionally thought to be produced by anaerobic archaeal methanogenesis in sediments where O_2 and SO_4^{2-} is depleted, but a substantial proportion of global marine CH_4 is produced in fully-oxygenated, high-SO_4^{2-} seawater (Repeta et al., 2016) and sediments (D'Hondt et al., 2002). Although SO_4^{2-}-reducing bacteria typically out-compete methanogens for substrates such as acetate (CH_3COO^-) or H_2, utilisation of non-competitive substrates by methanogens has been documented in many settings, allowing methanogenesis and sulfate reduction to occur simultaneously (Lazar et al., 2012; Mitterer et al., 2001; Oremland et al., 1982; Oremland and Polcin, 1982). Our bacterial and archaeal 16S rRNA show the co-occurrence of SO_4^{2-}-reducing bacteria, archaeal methanogens and anaerobic methanotrophic archaea within the first metre of sediment. This suggests that CH_4 and CO_2 (the latter via anaerobic oxidation of CH_4) are produced *in-situ* in the presence of seawater concentrations of SO_4^{2-} and active SO_4^{2-}-reducing bacteria. The main non-competitive substrates known are CH_3OH, methylamine (CH_3NH_2) and trimethylamine ($N(CH_3)_3$) (Finke et al., 2007). CH_3OH was a major compound in porewater dissolved organic matter from VC1 and VC2, in particular in the first 1 m of sediment (Fig. 5). At least one OTU from VC2 was potentially linked to methylotrophic methanogenesis (*Methanomassiliicoccaceae*).

Further microbial metabolism of dissolved porewater organics would proceed to form CO_2 and CH_4. In addition, while most metabolites we have detected are highly soluble in seawater, dimethyl sulfide (C_2H_6S) is

only slightly soluble in water. C_2H_6S is a degradation product of macroalgal organo-sulfur compounds (mainly dimethylsulfoniopropionate) or sulfur-containing amino acids (Kiene, 1988). C_2H_6S and methanethiol (CH_3SH) are important volatile components of the organic sulfur cycle and some of the most common gaseous compounds emitted from coastal marine environments (Bates et al., 1992; Visscher et al., 1995). We propose that C_2H_6S could be a potential microbial gaseous fluid from the Dunmanus Bay pockmark field. Microbial degradation of C_2H_6S (and other metabolites) and methylotrophic methanogenesis could produce CH_4 or CO_2. Given that the control site is characterized by a lower abundance of total organic matter input and more coarse-grained sandy sediment, differences in microbial activity and organic matter cycling is likely partly related to differences in hydrodynamic and depositional conditions, rather than unique microbial taxa or metabolic processes. However, could the *in-situ* production of gaseous microbial metabolites from consumption of labile sedimentary organic matter within surface sediments, result in the periodic low-scale seepage of gas and formation of small pockmarks? We hypothesize that heterotrophic microbial activity decomposing N- and S-containing labile organic matter can directly produce gas or be further oxidized to CO_2 or reduced to CH_4. Further investigation is needed to confirm this hypothesis and explore the extent to which this occurs in other settings. If confirmed, the contribution of greenhouse gases other than CH_4 from shallow water settings could be significantly underestimated.

5. Conclusions

In Dunmanus, pockmarks and associated sediments with previous acoustic evidence of gas accumulation display distinctly different sediment lithologies, organic matter supply and sedimentary biogeochemical processes. While bacterial community composition do not reveal unique taxa compared with control sediment, archaeal methanogens and anaerobic methanotrophic archaea were detected in sediments with highest CH_4. We also demonstrate much higher supply and turnover of labile organic matter, production of dissolved organic metabolites from N- and S-containing labile polymeric organic matter, and the accumulation of NH_4^+, PO_4^{3+} and H_2S from decomposition of these organics. Our data indicate significant NH_4^+ and H_2S production from complex proteins and hydrolyzed amino acids in porewater. The localised occurrence of fine-grained muddy sediments in areas with pockmarks indicate trapping and over-pressurization of fluid produces these small pockmarks. However, unlike other active seep sites, CH_4 was not present at concentrations high enough to produce gas bubbles, either in 2009 or 2011. This suggests gas accumulation and expulsion is temporally highly variable (over annual scales or less), and our surveys occurred during a quiescent period. Detected methanogens could also have been relatively inactive during the sampling period and/or CH_4 being produced could be efficiently oxidized to CO_2. Alternatively, acoustic signatures could be caused by a combination of fluids; we speculate that very shallow, *in situ* microbial processes can produce gaseous metabolites and by-products that directly contribute to pockmark formation. To fully test this hypothesis, further high-resolution and real-time monitoring of processes within and across bottom waters, surface and sub-surface sediments in pockmarks will be needed. Although unlikely to contribute to the formation of large pockmarks, similar microbial processes in surface sediments could contribute to formation of small pockmarks in favourable depositional conditions. Furthermore, microbial volatile organic compounds from shallow marine settings are clearly complex and could be underestimated in global atmospheric greenhouse gas inventories.

Author contributions

B.K., C.C.R.A. and A.J.S. guided experimental design. S.S.O'R, B.K., S.F.J and X.M. wrote the manuscript. A.J.S., R.S, B.W and A.J. designed and performed NMR experiments. S.S.O'R, S.F.J., X.M., S.G.M, M.T.S, AG DK and B.T.M. designed sampling surveys and carried out geochemical analysis. All authors discussed and independently interpreted the results and commented on the manuscript.

Declaration of competing interest

The authors declare that they have no known competing financial interests or personal relationships that could have appeared to influence the work reported in this paper.

Acknowledgements

The authors wish to thank the captain and crew of the RV Celtic Explorer. We would like to thank the Geological Survey of Ireland, the INFOMAR programme, Science Foundation Ireland Investigators Programme Award (16/IA/4520), iCRAG (SFI Research Centre) and the Irish Research Council for funding this research (2009 EMBARK, 2012 EMBARK and 2014 ELEVATE). We thank Carl G. Johnson (Woods Hole Oceanographic Institute, USA) for stable carbon isotope analysis of CH_4. We would also like to thank the anonymous reviewers whose input significantly improved this manuscript.

References

Anantharaman, K., Hausmann, B., Jungbluth, S.P., Kantor, R.S., Lavy, A., Warren, L.A., Rappé, M.S., Pester, M., Loy, A., Thomas, B.C., Banfield, J.F., 2018. Expanded diversity of microbial groups that shape the dissimilatory sulfur cycle. ISME J. 12, 1715–1728.

Baltzer, A., Ehrhold, A., Rigolet, C., Souron, A., Cordier, C., Clouet, H., Dubois, S.F., 2014. Geophysical exploration of an active pockmark field in the Bay of Concarneau, southern Brittany, and implications for resident suspension feeders. Geo Mar. Lett. 34, 215–230.

Bates, T.S., Lamb, B.K., Guenther, A., Dignon, J., 1992. Sulfur emissions to the atmosphere from natural sourees. Journal of Atmospheric 14, 315–337.

Batley, G.E., Simpson, S.L., 2009. Development of guidelines for ammonia in estuarine and marine water systems. Mar. Pollut. Bull. 58, 1472–1476.

Berry, D., Ben Mahfoudh, K., Wagner, M., Loy, A., 2011. Barcoded primers used in multiplex amplicon pyrosequencing bias amplification. Appl. Environ. Microbiol. 77, 7846–7849.

Boetius, A., Ravenschlag, K., Schubert, C.J., Rickert, D., Widdel, F., Gieseke, A., Amann, R., Jørgensen, B.B., Witte, U., Pfannkuche, O., 2000. A marine microbial consortium apparently mediating anaerobic oxidation of methane. Nature 407, 623–626.

Brothers, L.L., Kelley, J.T., Belknap, D.F., Barnhardt, W.A., Andrews, B.D., Maynard, M. L., 2011. More than a century of bathymetric observations and present-day shallow sediment characterization in Belfast Bay, Maine, USA: implications for pockmark field longevity. Geo Mar. Lett. 31, 237–248.

Cao, H., Zhang, W., Wang, Y., Qian, P.-Y., 2015. Microbial community changes along the active seepage site of one cold seep in the Red Sea. Front. Microbiol. 6, 739.

Christodoulou, D., Papatheodorou, G., Ferentinos, G., Masson, M., 2003. Active seepage in two constraining pockmark fields in the Patras and Corinth gulfs, Greece. Geo Mar. Lett. 23, 194–199.

Cline, J.D., 1969. Spectrophotometric determination OF hydrogen sulfide IN natural WATERS1. Limnol. Oceanogr. 14, 454–458.

Coughlan, M., Roy, S., O'Sullivan, C., Clements, A., O'Toole, R., Plets, R., 2021. Geological settings and controls of fluid migration and associated seafloor seepage features in the north Irish Sea. Mar. Petrol. Geol. 123, 104762.

D'Hondt, S., Rutherford, S., Spivack, A.J., 2002. Metabolic activity of subsurface life in deep-sea sediments. Science 295, 2067–2070.

Edwards, A., Jones, K., Graham, J.M., Griffiths, C.R., MacDougall, N., Patching, J., Richard, J.M., Raine, R., 1996. Transient coastal upwelling and water circulation in Bantry bay, a ria on the south-west coast of Ireland. Estuar. Coast Shelf Sci. 42, 213–230.

Fader, G.B.J., 1991. Gas-related sedimentary features from the eastern Canadian continental shelf. Continent. Shelf Res. 11, 1123–1153.

Farag, I.F., Davis, J.P., Youssef, N.H., Elshahed, M.S., 2014. Global patterns of abundance, diversity and community structure of the Aminicenantes (candidate phylum OP8). PloS One 9, e92139.

Fillol, M., Auguet, J.-C., Casamayor, E.O., Borrego, C.M., 2016. Insights in the ecology and evolutionary history of the Miscellaneous Crenarchaeotic Group lineage. ISME J. 10, 665–677.

Finke, N., Hoehler, T.M., Jørgensen, B.B., 2007. Hydrogen "leakage"during methanogenesis from methanol and methylamine: implications for anaerobic carbon degradation pathways in aquatic sediments. Environ. Microbiol. 9, 1060–1071.

Froelich, P.N., Klinkhammer, G.P., Bender, M.L., Luedtke, N.A., Heath, G.R., Cullen, D., Dauphin, P., Hammond, D., Hartman, B., Maynard, V., 1979. Early oxidation of organic matter in pelagic sediments of eastern equatorial Atlantic: suboxic diagenesis. Geochem. Cosmochim. Acta 43, 1075–1090.

Garcia-Gil, S., Vilas, F., Garcia-Garcia, A., 2002. Shallow gas features in incised-valley fills (Rıa de Vigo, NW Spain): a case study. Continent. Shelf Res. 22, 2303–2315.
Gardner, W.S., McCarthy, M.J., An, S., Sobolev, D., Sell, K.S., Brock, D., 2006. Nitrogen fixation and dissimilatory nitrate reduction to ammonium (DNRA) support nitrogen dynamics in Texas estuaries. Limnol. Oceanogr. 51, 558–568.
Giblin, A.E., Tobias, C.R., Song, B., Weston, N., Banta, G.T., Rivera-Monroy, V.H., 2013. The importance of dissimilatory nitrate reduction to ammonium (DNRA) in the nitrogen cycle of coastal ecosystems. Oceanography 26, 124–131.
Gonçalves, C.N., Dalmolin, R.S.D., Dick, D.P., Knicker, H., Klamt, E., Kögel-Knabner, I., 2003. The effect of 10% HF treatment on the resolution of CPMAS 13C NMR spectra and on the quality of organic matter in Ferralsols. Geoderma 116, 373–392.
Hamady, M., Walker, J.J., Harris, J.K., Gold, N.J., Knight, R., 2008. Error-correcting barcoded primers for pyrosequencing hundreds of samples in multiplex. Nat. Methods 5, 235–237.
Hammer, O., Harper, D.A.T., Ryan, P.D., 2001. Paleontological statistics software package for education and data analysis. Paleontologia Electronica 4, 9.
Harrington, P.K., 1985. Formation of pockmarks by pore-water escape. Geo Mar. Lett. 5, 193–197.
Hedberg, H.D., 1980. Methane Generation and Petroleum Migration.
Hedges, J.I., Keil, R.G., 1995. Sedimentary organic matter preservation: an assessment and speculative synthesis. Mar. Chem. 49, 81–115.
Hertkorn, N., Benner, R., Frommberger, M., Schmitt-Kopplin, P., Witt, M., Kaiser, K., Kettrup, A., Hedges, J.I., 2006. Characterization of a major refractory component of marine dissolved organic matter. Geochem. Cosmochim. Acta 70, 2990–3010.
Hovland, M., 1989. The formation of pockmarks and their potential influence on offshore construction. Q. J. Eng. Geol. Hydrogeol. 22, 131–138.
Hovland, M., 1981. Characteristics of pockmarks in the Norwegian trench. Mar. Geol. 39, 103–117.
Huettel, M., Ziebis, W., Forster, S., Luther, G.W., 1998. Advective transport affecting metal and nutrient distributions and interfacial fluxes in permeable sediments. Geochem. Cosmochim. Acta 62, 613–631.
Jordan, S.F., O'Reilly, S.S., Praeg, D., Dove, D., Facchin, L., Romeo, R., Szpak, M., Monteys, X., Murphy, B.T., Scott, G., McCarron, S.S., Kelleher, B.P., 2019. Geophysical and geochemical analysis of shallow gas and an associated pockmark field in Bantry Bay, Co. Cork, Ireland. Estuar. Coast Shelf Sci. 225, 106232.
Jørgensen, B.B., 1982. Mineralization of organic matter in the sea bed—the role of sulphate reduction. Nature 296, 643–645.
Jørgensen, B.B., 1977. The sulfur cycle of a coastal marine sediment (Limfjorden, Denmark) 1. Limnol. Oceanogr. 22, 814–832.
Judd, A.G., 2004. Natural seabed gas seeps as sources of atmospheric methane. Environ. Geol. 46, 988–996.
Judd, A.G., Croker, P., Tizzard, L., Voisey, C., 2007. Extensive methane-derived authigenic carbonates in the Irish Sea. Geo Mar. Lett. 27, 259–267.
Judd, A.G., Hovland, M., 2007. Seabed Fluid Flow: the Impact of Geology, Biology and the Marine Environment. Cambridge University Press, Cambridge, UK.
Kelleher, B.P., Simpson, A.J., Rogers, R.E., Dearman, J., Kingery, W.L., 2007. Effects of natural organic matter from sediments on the growth of marine gas hydrates. Mar. Chem. 103, 237–249.
Kiene, R.P., 1988. Dimethyl sulfide metabolism in salt marsh sediments. FEMS Microbiol. Ecol. 4, 71–78.
King, L.H., MacLean, B., 1970. Pockmarks on the scotian shelf. Geol. Soc. Am. Bull. 81, 3141–3148.
Knittel, K., Boetius, A., 2009. Anaerobic oxidation of methane: progress with an unknown process. Annu. Rev. Microbiol. 63, 311–334.
Krämer, K., Holler, P., Herbst, G., Bratek, A., Ahmerkamp, S., Neumann, A., Bartholomä, A., van Beusekom, J.E.E., Holtappels, M., Winter, C., 2017. Abrupt emergence of a large pockmark field in the German Bight, southeastern North Sea. Sci. Rep. 7, 5150.
Lam, B., Baer, A., Alaee, M., Lefebvre, B., Moser, A., Williams, A., Simpson, A.J., 2007. Major structural components in freshwater dissolved organic matter. Environ. Sci. Technol. 41, 8240–8247.
Lam, B., Simpson, A.J., 2008. Direct (1)H NMR spectroscopy of dissolved organic matter in natural waters. Analyst 133, 263–269.
Lazar, C.S., John Parkes, R., Cragg, B.A., L'Haridon, S., Toffin, L., 2012. Methanogenic activity and diversity in the centre of the amsterdam mud volcano, eastern mediterranean sea. FEMS Microbiol. Ecol. 81, 243–254.
Lloyd, K.G., Alperin, M.J., Teske, A., 2011. Environmental evidence for net methane production and oxidation in putative ANaerobic MEthanotrophic (ANME) archaea. Environ. Microbiol. 13, 2548–2564.
Lloyd, K.G., Schreiber, L., Petersen, D.G., Kjeldsen, K.U., Lever, M.A., Steen, A.D., Stepanauskas, R., Richter, M., Kleindienst, S., Lenk, S., Schramm, A., Jørgensen, B.B., 2013. Predominant archaea in marine sediments degrade detrital proteins. Nature 496, 215–218.
Missiaen, T., Murphy, S., Loncke, L., Henriet, J.-P., 2002. Very high-resolution seismic mapping of shallow gas in the Belgian coastal zone. Continent. Shelf Res. 22, 2291–2301.
Mitterer, R.M., Malone, M.J., Goodfriend, G.A., Swart, P.K., Wortmann, U.G., Logan, G. A., Feary, D.A., Hine, A.C., 2001. Co-generation of hydrogen sulfide and methane in marine carbonate sediments. Geophys. Res. Lett. 28, 3931–3934.
Miyatake, T., MacGregor, B.J., Boschker, H.T.S., 2009. Linking microbial community function to phylogeny of sulfate-reducing Deltaproteobacteria in marine sediments by combining stable isotope probing with magnetic-bead capture hybridization of 16S rRNA. Appl. Environ. Microbiol. 75, 4927–4935.
Nelson, H., Thor, D.R., Sandstrom, M.W., Kvenvolden, K.A., 1979. Modern biogenic gas-generated craters (sea-floor "pockmarks") on the Bering Shelf, Alaska. Geol. Soc. Am. Bull. 90, 1144–1152.
Nobu, M.K., Dodsworth, J.A., Murugapiran, S.K., Rinke, C., Gies, E.A., Webster, G., Schwientek, P., Kille, P., Parkes, R.J., Sass, H., Jørgensen, B.B., Weightman, A.J., Liu, W.-T., Hallam, S.J., Tsiamis, G., Woyke, T., Hedlund, B.P., 2016. Phylogeny and physiology of candidate phylum "Atribacteria" (OP9/JS1) inferred from cultivation-independent genomics. ISME J. 10, 273–286.
O'Reilly, S.S., Hryniewicz, K., Little, C.T.S., Monteys, X., Szpak, M.T., Murphy, B.T., Jordan, S.F., Allen, C.C.R., Kelleher, B.P., 2014. Shallow water methane-derived authigenic carbonate mounds at the Codling Fault Zone, western Irish Sea. Mar. Geol. 357, 139–150.
O'Reilly, S.S., Pentlavalli, P., Flanagan, P.V., Allen, C.C.R., Monteys, X., Szpak, M.T., Murphy, B.T., Jordan, S.F., Kelleher, B.P., 2016. Abundance and diversity of sedimentary bacterial communities in a coastal productive setting in the Western Irish Sea. Continent. Shelf Res. 113, 1–9.
Oremland, R.S., Marsh, L.M., Polcin, S., 1982. Methane production and simultaneous sulphate reduction in anoxic, salt marsh sediments. Nature 296, 143–145.
Oremland, R.S., Polcin, S., 1982. Methanogenesis and sulfate reduction: competitive and noncompetitive substrates in estuarine sediments. Appl. Environ. Microbiol. 44, 1270–1276.
Paull, C., Ussler III, W., Maher, N., Greene, H.G., Rehder, G., Lorenson, T., Lee, H., 2002. Pockmarks off big sur, California. Mar. Geol. 181, 323–335.
Phrampus, B.J., Lee, T.R., Wood, W.T., 2020. A global probabilistic prediction of cold seeps and associated SEAfloor FLuid expulsion anomalies (SEAFLEAs). G-cubed 21. https://doi.org/10.1029/2019GC008747.
Picard, K., Radke, L.C., Williams, D.K., Nicholas, W.A., Siwabessy, P.J., Howard, F.J.F., Gafeira, J., Przeslawski, R., Huang, Z., Nichol, S., 2018. Origin of high density seabed pockmark fields and their use in inferring bottom currents. Geosci. J. 8, 195.
Pickrill, R.A., 2006. Shallow seismic stratigraphy and pockmarks of a hydrothermally influenced lake, Lake Rotoiti, New Zealand. Sedimentology 40, 813–828.
Pilcher, R., Argent, J., 2007. Mega-pockmarks and linear pockmark trains on the West African continental margin. Mar. Geol. 244, 15–32.
Reeburgh, W.S., 2007. Oceanic methane biogeochemistry. Chem. Rev. 107, 486–513.
Repeta, D.J., Ferrón, S., Sosa, O.A., Johnson, C.G., Repeta, L.D., Acker, M., DeLong, E.F., Karl, D.M., 2016. Marine methane paradox explained by bacterial degradation of dissolved organic matter. Nat. Geosci. 9, 884–887.
Sansone, F.J., Martens, C.S., 1982. Volatile fatty acid cycling in organic-rich marine sediments. Geochem. Cosmochim. Acta 46, 1575–1589.
Santos, I.R., Eyre, B.D., Huettel, M., 2012. The driving forces of porewater and groundwater flow in permeable coastal sediments: a review. Estuar. Coast Shelf Sci. 98, 1–15.
Schubel, J.R., 1974. Gas bubbles and the acoustically impenetrable, or turbid, character of some estuarine sediments. In: Kaplan, I.R. (Ed.), Natural Gases in Marine Sediments. Springer US, Boston, MA, pp. 275–298.
Schulz, H.D., Dahmke, A., Schinzel, U., Wallmann, K., Zabel, M., 1994. Early diagenetic processes, fluxes, and reaction rates in sediments of the South Atlantic. Geochem. Cosmochim. Acta 58, 2041–2060.
Simpson, A.J., Brown, S.A., 2005. Purge NMR: effective and easy solvent suppression. J. Magn. Reson. 175, 340–346.
Simpson, A.J., Simpson, M.J., Smith, E., Kelleher, B.P., 2007. Microbially derived inputs to soil organic matter: are current estimates too low? Environ. Sci. Technol. 41, 8070–8076.
Skarke, A., Ruppel, C., Kodis, M., Brothers, D., Lobecker, E., 2014. Widespread methane leakage from the sea floor on the northern US Atlantic margin. Nat. Geosci. 7, 657–661.
Sørensen, J., Christensen, D., Jørgensen, B.B., 1981. Volatile Fatty acids and hydrogen as substrates for sulfate-reducing bacteria in anaerobic marine sediment. Appl. Environ. Microbiol. 42, 5–11.
Stolper, D.A., Martini, A.M., Clog, M., Douglas, P.M., Shusta, S.S., Valentine, D.L., Sessions, A.L., Eiler, J.M., 2015. Distinguishing and understanding thermogenic and biogenic sources of methane using multiply substituted isotopologues. Geochem. Cosmochim. Acta 161, 219–247.
Stott, L., Davy, B., Shao, J., Coffin, R., Pecher, I., Neil, H., Rose, P., Bialas, J., 2019. CO 2 release from pockmarks on the chatham rise-bounty trough at the glacial termination. Paleoceanography and Paleoclimatology, Geophysical Monograph Series 34, 1726–1743.
Szpak, M.T., Monteys, X., O'Reilly, S., Simpson, A.J., Garcia, X., Evans, R.L., Allen, C.C. R., McNally, D.J., Courtier-Murias, D., Kelleher, B.P., 2012. Geophysical and geochemical survey of a large marine pockmark on the Malin Shelf, Ireland. G-cubed 13.
Szpak, M.T., Monteys, X., O'Reilly, S.S., Lilley, M.K.S., Scott, G.A., Hart, K.M., McCarron, S.G., Kelleher, B.P., 2015. Occurrence, characteristics and formation mechanisms of methane generated micro-pockmarks in Dunmanus Bay, Ireland. Continent. Shelf Res. 103, 45–59.
Towns, T.G., 1986. Determination of aqueous phosphate by ascorbic acid reduction of phosphomolybdic acid. Anal. Chem. 58, 223–229.
Valentine, D.L., Reeburgh, W.S., 2000. New perspectives on anaerobic methane oxidation. Environ. Microbiol. 2, 477–484.
Vanwonterghem, I., Evans, P.N., Parks, D.H., Jensen, P.D., Woodcroft, B.J., Hugenholtz, P., Tyson, G.W., 2016. Methylotrophic methanogenesis discovered in the archaeal phylum Verstraetearchaeota. Nat Microbiol 1, 16170.
Vetriani, C., Jannasch, H.W., MacGregor, B.J., Stahl, D.A., Reysenbach, A.L., 1999. Population structure and phylogenetic characterization of marine benthic Archaea in deep-sea sediments. Appl. Environ. Microbiol. 65, 4375–4384.
Vigneron, A., Alsop, E.B., Cruaud, P., Philibert, G., King, B., Baksmaty, L., Lavallée, D., P Lomans, B., Kyrpides, N.C., Head, I.M., Tsesmetzis, N., 2017. Comparative metagenomics of hydrocarbon and methane seeps of the Gulf of Mexico. Sci. Rep. 7, 16015.

Visscher, P.T., Taylor, B.F., Kiene, R.P., 1995. Microbial consumption of dimethyl sulfide and methanethiol in coastal marine sediments. FEMS Microbiol. Ecol. 18, 145–153.
Wang, Y., Gao, Z.-M., Li, J.-T., Bougouffa, S., Tian, R.M., Bajic, V.B., Qian, P.-Y., 2016. Draft genome of an Aerophobetes bacterium reveals a facultative lifestyle in deep-sea anaerobic sediments. Sci. Bull. Facul. Agric. Kyushu Univ. 61, 1176–1186.
Weber, T., Wiseman, N.A., Kock, A., 2019. Global ocean methane emissions dominated by shallow coastal waters. Nat. Commun. 10, 4584.
Whiticar, M.J., 1999. Carbon and hydrogen isotope systematics of bacterial formation and oxidation of methane. Chem. Geol. 161, 291–314.
Wildish, D.J., Akagi, H.M., McKeown, D.L., Pohle, G.W., 2008. Pockmarks influence benthic communities in passamaquoddy bay, bay of fundy, Canada. Mar. Ecol. Prog. Ser. 357, 51–65.
Wirth, S.B., Bouffard, D., Zopfi, J., 2020. Lacustrine groundwater discharge through giant pockmarks (lake neuchatel, Switzerland). Frontiers in Water 2, 13.
Wu, D.H., Chen, A.D., Johnson, C.S., 1995. An improved diffusion-ordered spectroscopy experiment incorporating bipolar-gradient pulses. J. Magn. Reson. 115, 260–264.